Simplified method for including spatial correlations in mean-field approximations

Deborah C. Markham,[1,*] Matthew J. Simpson,[2] and Ruth E. Baker[1]

[1]*Centre for Mathematical Biology, Mathematical Institute, University of Oxford, 24-29 St Giles', Oxford OX1 3LB, United Kingdom*

[2]*School of Mathematical Sciences, Queensland University of Technology, G.P.O. Box 2434, Brisbane, Queensland 4001, Australia*

(Received 13 March 2013; published 10 June 2013)

Biological systems involving proliferation, migration, and death are observed across all scales. For example, they govern cellular processes such as wound healing, as well as the population dynamics of groups of organisms. In this paper, we provide a simplified method for correcting mean-field approximations of volume-excluding birth-death-movement processes on a regular lattice. An initially uniform distribution of agents on the lattice may give rise to spatial heterogeneity, depending on the relative rates of proliferation, migration, and death. Many frameworks chosen to model these systems neglect spatial correlations, which can lead to inaccurate predictions of their behavior. For example, the logistic model is frequently chosen, which is the mean-field approximation in this case. This mean-field description can be corrected by including a system of ordinary differential equations for pairwise correlations between lattice site occupancies at various lattice distances. In this work we discuss difficulties with this method and provide a simplification in the form of a partial differential equation description for the evolution of pairwise spatial correlations over time. We test our simplified model against the more complex corrected mean-field model, finding excellent agreement. We show how our model successfully predicts system behavior in regions where the mean-field approximation shows large discrepancies. Additionally, we investigate regions of parameter space where migration is reduced relative to proliferation, which has not been examined in detail before and find our method is successful at correcting the deviations observed in the mean-field model in these parameter regimes.

DOI: 10.1103/PhysRevE.87.062702 PACS number(s): 87.10.Ed, 87.10.Hk, 87.10.Mn

I. INTRODUCTION

Throughout biology, we frequently observe spatial correlations in the distribution of individual entities. For example, in an infectious epidemic we see correlations between the distribution of infected individuals, which affects transmission of the disease [1–5]. At a different level, microbes in soil have been shown to have correlations in their spatial distributions not only at the microscale in the topsoil but also on the scale of meters in the subsoil [6]. In cancerous human brains, applying spatial statistics to histological images has shown glioma cells to have spatial correlations at intermediate and large distances [7]. Moreover, different spatial distributions of individuals can lead to different behavior. For instance, it has been shown that clusters of bacteria can initiate human blood coagulation, whereas the same amount of bacteria distributed evenly will not initiate coagulation as rapidly [8]. Thus, to provide robust models of biological systems, it is essential that we are able to incorporate the effects of spatial correlations.

Individual-based models (IBMs), such as cellular automata, are generally able to reproduce these observed correlations [9–11]. On the other hand, mean-field approximations (MFAs), such as the logistic model, consider only total density as a function of time and typically neglect spatial correlations, potentially leading to inaccurate representations of the systems under study [12–14]. Simulating IBMs is a useful step in modeling biological processes; however, they are generally not suitable as the sole method of investigation as they are computationally expensive. This often makes it impossible to simulate realistically sized systems and means that it is challenging to thoroughly investigate the parameter space, especially as many realizations need to be performed to obtain reliable statistics. Thus, it is desirable to have a continuum description to complement models at the individual level, as these are far less computationally expensive to investigate numerically. Moreover, they are generally more amenable to mathematical analysis which can provide valuable insight regarding the behavior in different regions of parameter space. However, if the continuum description does not take into account spatial correlations, it may not accurately encode individual behaviors, thus potentially disagreeing with the averaged IBM results. Therefore it is necessary to have methods for including spatial correlations in the continuum description of a system.

We can include spatial correlations using pairwise approximations, as in Refs. [4,5,15–27]. In Ref. [15], the authors showed how correcting the MFA using correlation functions led to closer agreement with the results of averaged discrete simulations for a volume-excluding system on a regular lattice, whereby agents underwent proliferation, movement, and death. Processes of nearest-neighbor proliferation and death on a regular grid are frequently referred to as contact processes, which were initially developed to describe the spread of epidemics [28,29]. When movement is included, they are then known as contact processes with diffusion [30,31].

The technique introduced by Baker and Simpson [15] has been extended to include inhomogeneous initial conditions, allowing for the examination of moving fronts [20]. Moreover, it has recently been used to calibrate experimental data from two different cell types in comparison with the MFA [32]. The authors show that the cells with greater motility are adequately represented by the MFA, whereas the less motile cell type requires the more sophisticated model, which includes correlations, to accurately predict evolution of the

*markham@maths.ox.ac.uk

population. The use of spatial statistics has shown how it may be possible to decide where the MFA breaks down, avoiding costly errors when calibrating data.

A difficulty encountered using the approach of Ref. [15] to correct the MFA in higher dimensions [two dimensions (2D) and three dimensions (3D)] is the numerical expense of encoding, into the system of ordinary differential equations (ODEs), descriptions of the correlations at the various lattice distances. In an effort to tackle this problem, studies have also been carried out to provide a partial differential equation (PDE) description of nearest-neighbor two-point correlations for an invasion problem with adhesion and contact interactions [21]. However, spatial correlations are not necessarily confined to nearest-neighbor pairs, something this approach cannot account for. A PDE description of spatial correlations exists for off-lattice point-particle (nonexcluding) models [23]; however, its parameters must be obtained from averaged discrete simulations, thus it cannot stand alone. As such, inclusion of the effects of spatial correlations into such models in a tractable way remains an unanswered question.

In this paper, we show how to extend the model in Ref. [15], and increase its usability, by constructing a PDE description of the system of ODEs describing spatial correlations. Additionally, we investigate a wider parameter regime, taking into account regions of parameter space where motility is reduced relative to proliferation. Biologically, this has been observed in some forms of cancer where cells are proliferating rapidly but do not have high levels of motility [33]. This region of parameter space may also be important for modeling plant dynamics, where movement generally does not feature [34,35].

In Sec. II, we describe how to derive equations for the evolution of spatial correlations for various distances on a regular lattice. Results comparing predictions from the logistic equation, the correlation-corrected logistic equation and the averaged results from the IBM show how the inclusion of pairwise correlations allows for better approximation of the averaged individual-level behavior. We then discuss the practical difficulties with using these methods, which we ameliorate by developing a PDE representation of the correlation functions in Sec. III. We next, in Sec. IV, investigate reducing motility rates relative to proliferation rates. Finally, in Sec. V, we conclude our work and discuss future directions.

II. DERIVING THE EVOLUTION OF CORRELATION FUNCTIONS

In this section, we briefly discuss the system in question and how the correlation ODEs are derived. We also show how correlation ODEs provide a better agreement with IBMs than does the MFA and discuss difficulties encountered using this method.

A. Outline of the system

We consider a d-dimensional system on a regular, square lattice with lattice spacing Δ. Initially, agents are placed randomly on the lattice with each site having an occupancy probability of P_i; therefore, we have homogeneous initial conditions. We regard sites as being occupied (state A) or unoccupied (state 0), with the lattice state of site l being described by the variable σ_l. The normalized average agent density is denoted by $c_A(t)$ as follows:

$$c_A(t) = \frac{1}{N_{\text{tot}}} \sum_i \mathbb{1}_A\{\sigma_i\}, \tag{2.1}$$

where N_{tot} is the total number of lattice sites and $\mathbb{1}_A$ is the indicator function. The agents move to neighboring lattice sites with a probability P_m per unit time; they proliferate and place a daughter on a neighboring lattice site with a probabilty P_p per unit time and die with a probability P_d per unit time. Proliferation and movement will occur only if the target site is unoccupied, thereby giving rise to volume exclusion, and the target site is chosen at random from the nearest-neighbor sites. In Fig. 1, we show how individual simulations with homogeneous initial conditions display a buildup of spatial correlations, which is evident by the increasing patchiness.

B. Evolution of correlation functions

We will now briefly discuss the derivation of the evolution of spatial correlations; we refer the reader to Ref. [15] for a more in-depth derivation. First, we define the k-point distribution functions, $\rho^{(k)}$, as the probability that k sites have given occupancies. For example, $\rho^{(2)}(A_l, A_m)$ is the probability that sites l and m are both in state A. Due to the homogeneous initial conditions, $\rho^{(1)}(A_l)$ is the cell density, c_A, defined in

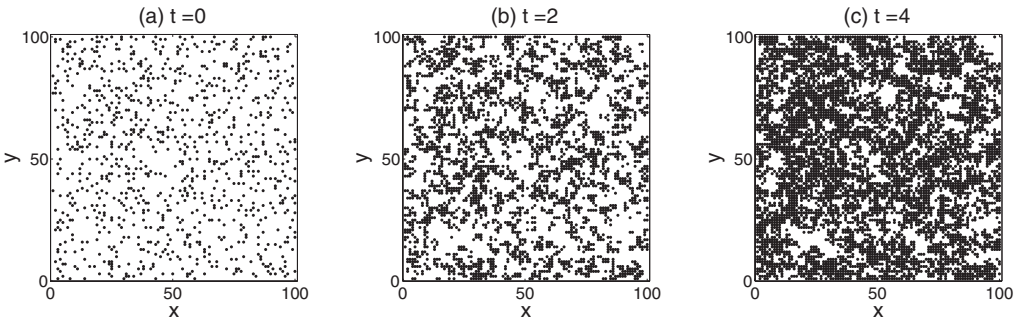

FIG. 1. We see that spatial correlations, as evident by the patchiness, build up over time from homogeneous (spatially uniform) initial conditions. Results here are in 2D on a 100×100 lattice for parameters $P_m = 0.5$, $P_p = 1.0$, $P_d = 0.1$, and $P_i = 0.1$. Details of the numerical algorithm can be found in Sec. II C.

Eq. (2.1). Next, we define our correlation functions [36,37] as

$$F_{\lambda,\mu}(|\mathbf{l}-\mathbf{m}|) := \frac{\rho^{(2)}(\sigma_l,\sigma_m)}{\rho^{(1)}(\sigma_l)\rho^{(1)}(\sigma_m)} = \frac{\rho^{(2)}(\sigma_l,\sigma_m)}{c_\lambda c_\mu}, \tag{2.2}$$

where λ and μ denote the states of sites $\mathbf{l}$ and $\mathbf{m}$, respectively. Note that the correlation functions depend only on the distances between the lattice sites, due to the homogeneous initial conditions, and this leads to radial symmetry and translational invariance on the lattice. If each site occupancy is independent of the occupancies of all other sites, the correlation functions are unity. By obtaining a master equation for the evolution of the one-point distribution function, it is possible to obtain an expression for the evolution of the cell density as follows:

$$\frac{dc_A}{dt} = P_p c_A[1 - F_{A,A}(\Delta)c_A] - P_d c_A. \tag{2.3}$$

We observe that if lattice site occupancies are independent, $F_{A,A}(\Delta) = 1$, the equation reduces to

$$\frac{dc_A}{dt} = P_p c_A(1 - c_A) - P_d c_A, \tag{2.4}$$

which is simply the (unscaled) logistic equation, the MFA expected in this system. Using the two-point distribution function, and the definition of a correlation function, we can obtain an expression for the evolution of the correlation functions. This equation includes $\rho^{(3)}$ terms; thus, we need an appropriate closure approximation in order to close the system. We use the Kirkwood superposition approximation (KSA), as chosen in Ref. [15],

$$\rho^{(3)}(\sigma_l,\sigma_m,\sigma_n) = \frac{\rho^{(2)}(\sigma_l,\sigma_m)\rho^{(2)}(\sigma_l,\sigma_n)\rho^{(2)}(\sigma_m,\sigma_n)}{\rho^{(1)}(\sigma_l)\rho^{(1)}(\sigma_m)\rho^{(1)}(\sigma_n)}. \tag{2.5}$$

There are, of course, other closures, such as those found in Ref. [24], but we found that the KSA consistently performs best (results not shown), which can be explained by the fact it maximizes the entropy of the system [27,38]. Using this closure, we obtain the following equation for the evolution of the correlation functions as follows:

$$\begin{aligned}
&\frac{dF_{A,A}}{dt}(|\mathbf{l}-\mathbf{m}|) \\
&= \frac{P_m}{d}\sum_{n\neq l}\alpha_{n,m}[F_{A,A}(|\mathbf{l}-\mathbf{n}|) - F_{A,A}(|\mathbf{l}-\mathbf{m}|)] \\
&\quad + \frac{P_p}{d(1-c_A)}[1 - c_A F_{A,A}(|\mathbf{l}-\mathbf{m}|)][1 - c_A F_{A,A}(\Delta)] \\
&\quad \times \left[\sum_{n\neq l}\alpha_{n,m}F_{A,A}(|\mathbf{l}-\mathbf{n}|)\right] + \frac{P_p}{dc_A}\alpha_{l,m}[1 - c_A F_{A,A}(\Delta)] \\
&\quad - 2P_p[1 - c_A F_{A,A}(\Delta)]F_{A,A}(|\mathbf{l}-\mathbf{m}|),
\end{aligned} \tag{2.6}$$

where $\alpha_{n,m} = 1$ if n and m are nearest neighbors (in a von Neumann neighborhood) and otherwise it is zero. The number of spatial dimensions in the system is given by d.

C. Testing the performance of the correlation functions

We now compare results from simulations including correlations with the MFA and the averaged IBM. For the MFA, we solve the ODE in Eq. (2.4) using a standard fourth-order Runge-Kutta method [39] with a constant time step of $\delta t = 0.1$ (smaller time steps were tested in order to confirm this was an appropriate choice). For the case where correlations are included, we need to solve a large system of ODEs. This system is composed of Eq. (2.3) and the family of equations given in Eq. (2.6), where there is one ODE for every distance on the lattice. Note that we only need to take into account the distance between lattice sites as the system is radially symmetric and translationally invariant due to the homogeneous initial conditions. The correlation ODEs differ for each distance on the lattice in 2D and 3D due to the nonuniformity of the radial distance on a square lattice. Thus, for practical reasons, we need to truncate after a sufficiently large distance and assume lattice sites are independent ($F_{A,A}(|\mathbf{l}-\mathbf{m}|) = 1$) beyond this distance, generally taken to be 3Δ here. Ideally, we would like to truncate at a higher distance but this is not practically feasible, particularly in 3D. Again, the ODEs are solved using a fourth-order Runge-Kutta method.

For our discrete simulations, we use a regular square lattice of size $N_x \times N_y = 100 \times 100$ in 2D, $N_x \times N_y \times N_z = 20 \times 20 \times 20$ in 3D, to give approximately the same number of total lattice sites in each system. The boundary conditions are periodic, and we have random initial conditions. For all results shown here, $P_i = 0.1$. However, the results shown in the work also apply for different initial conditions, which were examined thoroughly in previous work [15]. We average over 100 simulations of our IBM and compare to our continuum approximations. A modified Gillespie approach is used for our discrete realisations, as described in Ref. [15].

When plotting our results, we rescale time and density to compare different proliferation and death rates. We rescale time by

$$\bar{t} = (P_p - P_d)t \tag{2.7}$$

and density by

$$\bar{c}_A = \left(\frac{P_p - P_d}{P_p}\right)c_A. \tag{2.8}$$

As seen in Fig. 2, inclusion of the system of ODEs incorporating correlations provides a better approximation to the averaged discrete system than does the MFA, suggesting that correlations should be taken into account when predicting IBM behavior. However, there are some difficulties with using this method. In 2D and 3D, the distances between lattice sites are nonuniform. For example, in 2D, the correlation function at a radial distance of 2Δ will depend on the correlation functions at distances of 3Δ and $\sqrt{5}\Delta$, while the correlation function at a radial distance of 3Δ will depend on 2Δ, $\sqrt{10}\Delta$, and 4Δ. It is time-consuming in practice to calculate the distances of the nearest-neighbors for each radial distance, $|\mathbf{l}-\mathbf{m}|$, and to encode this information in order to solve the system numerically. However, this problem could be overcome by developing a PDE approximation for the system of correlation function ODEs. The PDE would be much simpler to solve, as using a regular lattice would now be possible, making applications of this method more feasible. It would also ensure we do not assume lattice site independence prematurely, as it is straightforward to test different truncation distances. It is to this problem that we now turn.

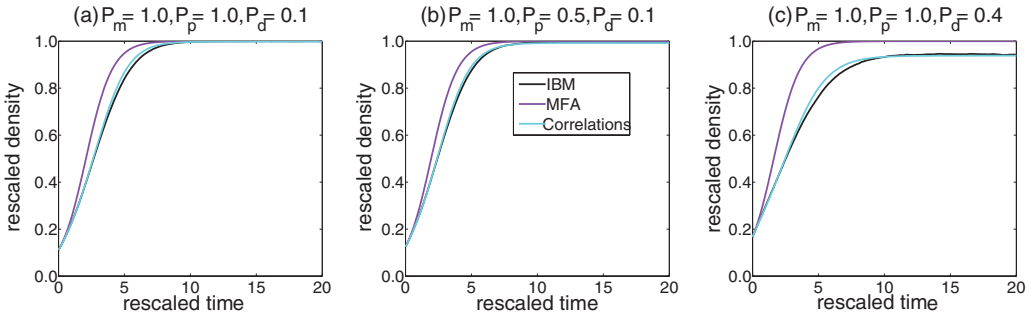

FIG. 2. (Color online) Including pairwise correlations, as in Eq. (2.6), provides much better agreement with the results of averaged discrete simulations than using the MFA does. The results shown here are for a 2D system. Results for a range of parameters in both 2D and 3D can be found in Ref. [15].

III. DERIVING THE PDE

In this section, we describe how to obtain a PDE representation of the correlation ODEs in 2D and 3D. The distance between lattice sites increases irregularly ($\Delta, \sqrt{2}\Delta, 2\Delta, \sqrt{5}\Delta$, etc., in 2D), and the neighbors for each site have to be calculated separately for each distance. This is inconvenient, and, thus, a PDE description of the correlation functions would be a huge advantage. As Δ is a small parameter relative to the system size, we use Taylor series expansions of the correlation functions around the site located at a distance $|\mathbf{l}-\mathbf{m}|$. Biologically, Δ corresponds to the diameter of a cell, thus, we anticipate our approximation to be valid on length scales greater than that of a single lattice site. We derive and test the PDE approximation in 2D and then extend our methods to 3D.

A. Derivation in two dimensions

Due to the homogeneous initial conditions, we need only consider correlation functions for sites a radial distance s apart rather than each pair of points on the lattice. However, in order to develop a PDE approximation, it is more convenient to express our correlation functions in terms of Cartesian coordinates (x and y in 2D and x, y, and z in 3D) of our lattice site at radial distance $|\mathbf{l}-\mathbf{m}|$. This allows us to write all the equations for evolution of the correlation functions, apart from when the lattice distance is one cell, in the same form. We can then use Taylor-series expansions to approximate the system of ODEs by a PDE. A boundary condition on our PDE will be given at a radial distance of one cell diameter (Δ). This boundary condition, from Eq. (2.6), is given by

$$\frac{dF(\Delta)}{dt} = \frac{P_m}{2}[2F(\sqrt{2}\Delta) + F(2\Delta) - 3F(\Delta)] - 2P_pF(\Delta)[1-c_AF(\Delta)] + \frac{P_p}{2c_A}[1-c_AF(\Delta)] + \frac{P_p}{2(1-c_A)}[1-c_AF(\Delta)]^2[2F(\sqrt{2}\Delta) + F(2\Delta)]. \tag{3.1}$$

The Cartesian coordinate representation for the rest of the correlation functions is given by

$$\frac{dF(x,y)}{dt} = \frac{P_m}{2}[F(x+\Delta,y) + F(x-\Delta,y) + F(x,y+\Delta) + F(x,y-\Delta) - 4F(x,y)] - 2P_pF(x,y)[1-c_AF(\Delta)] + \frac{P_p}{2(1-c_A)}[1-c_AF(\Delta)][1-c_AF(x,y)][F(x+\Delta,y) + F(x-\Delta,y) + F(x,y+\Delta) + F(x,y-\Delta)], \tag{3.2}$$

where $\sqrt{x^2+y^2} > \Delta$. We perform a 2D Taylor-series expansion of Eq. (3.2) around (x,y), keeping terms up to second order to obtain

$$\frac{\partial F(x,y)}{\partial t} = \frac{P_m\Delta^2}{2}\left[\frac{\partial^2F(x,y)}{\partial x^2} + \frac{\partial^2F(x,y)}{\partial y^2}\right] - 2P_pF(x,y)[1-c_AF(\Delta)] + \frac{P_p}{2(1-c_A)}[1-c_AF(\Delta)][1-c_AF(x,y)] \times \left[4F(x,y) + \Delta^2\frac{\partial^2F(x,y)}{\partial x^2} + \Delta^2\frac{\partial^2F(x,y)}{\partial y^2}\right] + \mathcal{O}(\Delta^3). \tag{3.3}$$

Due to the choice of homogeneous initial conditions, our system is radially symmetric and translationally invariant, thus, we can reduce the complexity by switching to radial coordinates as follows:

$$\frac{\partial F(s)}{\partial t} = \frac{P_m\Delta^2}{2}\left[\frac{\partial^2F(s)}{\partial s^2} + \frac{1}{s}\frac{\partial F(s)}{\partial s}\right] - 2P_pF(s)[1-c_AF(\Delta)] + \frac{P_p}{2(1-c_A)}[1-c_AF(\Delta)][1-c_AF(s)]\left[4F(s) + \Delta^2\frac{\partial^2F}{\partial s^2} + \Delta^2\frac{1}{s}\frac{\partial F}{\partial s}\right], \qquad s > \Delta, \tag{3.4}$$

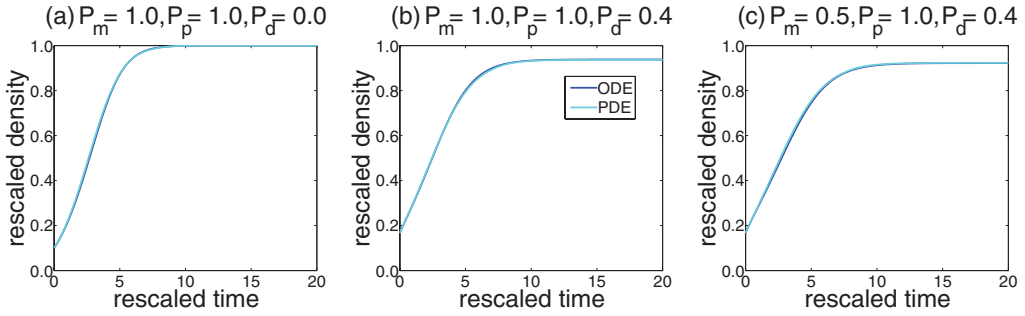

FIG. 3. (Color online) Comparing the PDE approximation, Eqs. (3.1) and (3.6), to the system of ODEs, Eq. (2.6), in 2D. We observe that the PDE provides excellent agreement with the system of ODEs, being virtually indistinguishable visually.

where s is the radial distance between two lattice sites. Generally, in obtaining a PDE, we now take the limit as $\Delta \to 0$ [40–44]. At this point, it is important to consider how P_m will change if Δ is modified. P_m has been chosen as the rate at which an agent will attempt to move to an unoccupied neighboring lattice site. We notice that if P_m does not scale with Δ^2, we will lose our movement terms entirely, thus, we expect $P_m\Delta^2$ to remain constant, in keeping with other PDE derivations that do not incorporate correlations [40–44]. This can be expressed as

$$\hat{P}_m = P_m\Delta^2. \tag{3.5}$$

In our discrete simulations we have taken $\Delta = 1$, thus, $\hat{P}_m = P_m$. For different values of Δ, $\hat{P}_m$ can be obtained using Eq. (3.5). On taking the limit as $\Delta \to 0$, we obtain the following PDE:

$$\frac{\partial F(s)}{\partial t} = \frac{\hat{P}_m}{2}\left[\frac{\partial^2 F(s)}{\partial s^2} + \frac{1}{s}\frac{\partial F(s)}{\partial s}\right] + 2P_p c_A F(s)\left[1 - c_A F(\Delta)\right]\left[\frac{1 - F(s)}{1 - c_A}\right], \quad s > \Delta. \tag{3.6}$$

Note that we explicitly retain the boundary Eq. (3.1) in our system, since we expect our approximation, Eq. (3.6), to be valid only over length scales greater than a single lattice site. We expect the correlations to decay in the limit of large lattice spacing; thus, the boundary condition at large distances is given by

$$F(s \to \infty) = 1, \tag{3.7}$$

meaning that the occupancies of distant sites are uncorrelated.

We test our PDE approximation in 2D, Eqs. (3.1) and (3.6), by comparing it to results from solving the system of correlation ODEs given by Eq. (2.6). To solve our PDE system numerically, we now have to consider two ODEs (one for the cell density and one for correlations at the nearest-neighbor distance) and a PDE. In order to solve our PDE numerically we use a backwards Euler method and solve the resulting nonlinear algebraic equations using the tridiagonal matrix algorithm [39] with Picard iteration [45]. We use a time step of $\delta t = 0.1$ and a space step of $\delta x = 0.01$. Again, smaller values were tested to ensure these were appropriately selected. We terminate our PDE domain at a distance of 20Δ, assuming all sites further apart are independent. We confirmed this assumption for all cases by solving our PDE on larger domains and ensuring visually indistinguishable results were obtained. We find that the PDE consistently provides a reliable approximation to the correlation ODEs, illustrated in Fig. 3.

We observe that Eq. (3.6) has the form of a reaction-diffusion equation. The diffusion coefficient depends only on P_m and we see that correlations will decay faster by the diffusive term if P_m is increased. This agrees with our intuition, as we would expect higher rates of movement to break up clusters of agents. We observe in Fig. 4 that increasing P_m for a constant P_p (in the absence of agent death) causes correlations to decay faster. When P_m is smaller, the correlation functions have a greater maximum, which is to be expected due to the slower dispersal.

Our "reaction" term in Eqs. (3.6) is given by

$$2P_p c_A[1 - c_A F(\Delta)]\left[\frac{1 - F(s)}{1 - c_A}\right]. \tag{3.8}$$

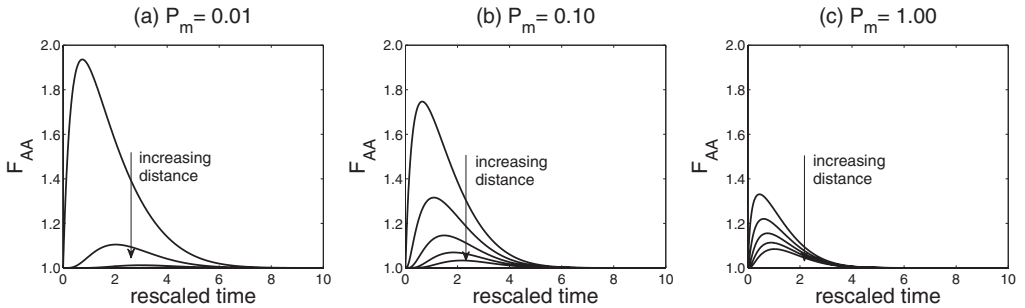

FIG. 4. Increasing the movement rate, P_m, causes the pairwise correlation functions, Eq. (3.6), to decay faster. The distance, s, increases from Δ to 3Δ in steps of 0.5Δ. These results are in 2D for $P_p = 0.1$ and $P_d = 0$.

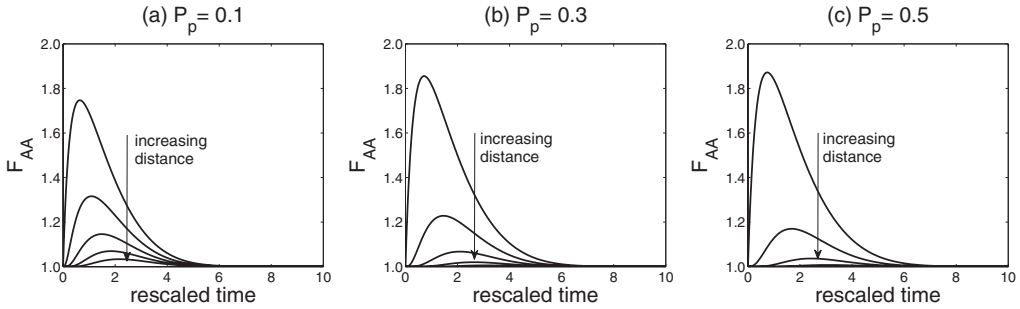

FIG. 5. Increasing the proliferation rate, P_p, causes an increase in the pairwise correlation functions at the boundary ($s = \Delta$) but a decrease in the correlation functions at larger distances, $s > \Delta$. The distance, s, increases from Δ to 3Δ in steps of 0.5Δ. Results shown are in 2D for $P_m = 0.1$ and $P_d = 0$.

We see that the reaction term depends on the rate of proliferation; however, it is unclear whether this term is positive or negative. We know that $2P_p c_A$ will always be positive by definition. We next examine the fraction $(1 - F(s))/(1 - c_A)$, noting that the denominator is always positive as $c_A \leqslant 1$ by definition. The correlation function, $F(s)$, is unity if sites are uncorrelated. If sites are correlated, $F(s) > 1$ and if sites are negatively correlated, $F(s) < 1$. In our system, sites cannot become negatively correlated as this would only happen if, for instance, cells were more likely to die when they were surrounded by other cells. Thus, $F(s) \geqslant 1$. Therefore, we expect $(1 - F(s))/(1 - c_A)$ to be nonpositive. Finally, the remaining component of our reaction term is $[1 - c_A F(\Delta)]$. To determine the sign of this, we need to determine the magnitude of $c_A F(\Delta)$. Remembering our definition of the correlation function, we can rewrite this as $\rho^{(2)}(A_l, A_{l+\Delta})/c_A$. The numerator of this will always be less than or equal to the denominator because of the following conservation statement:

$$\rho^{(2)}(A_l, A_m) + \rho^{(2)}(A_l, 0_m) = \rho^{(1)}(A_l) = c_A. \qquad (3.9)$$

Therefore, $c_A F(\Delta) \leqslant 1$ and $[1 - c_A F(\Delta)] \geqslant 0$. This means that our reaction term will never be positive. Therefore, an increase in P_p will lead to a decrease in correlations for that specific distance. At first, this seems counterintuitive as we expect an increase in the proliferation rate to cause a buildup of correlations. However, this can be explained by considering the effect on the one-point and two-point distribution functions. A proliferation event at site l will increase the total agent density, c_A. It will not necessarily increase the two-point distribution function for lattice sites at distance $l > \Delta$ apart. The correlation function is proportional to the two-point distribution function and inversely proportional to the squared one-point distribution function. Therefore, we expect the correlation function at this specific distance to decrease, as the one-point distribution function will definitely increase. We also note that at the boundary of our correlation PDE, in the expression for the evolution of $F(\Delta)$, Eq. (3.1), proliferation can have an overall positive effect on the buildup of correlations. We can think of the boundary condition in the PDE as acting as a source of correlations which then get dispersed by movement. This phenomenon occurs as we only consider nearest-neighbor proliferation mechanisms. In Fig. 5, we see that increasing P_p, while keeping P_m constant, leads to an increase in the correlation function at the boundary ($s = \Delta$) but a decrease in the correlation function at all other distances.

Using a PDE approximation also enables us to examine the behavior of the correlation function as a function of distance, as shown in Fig. 6. As we expect, the correlation function decreases as the distance increases, reaching a steady state of unity, confirming Eq. (3.7). We see, especially at later times, that the correlation function does not reach a steady state until approximately 10Δ, which would involve a large number of coupled ODEs in the previous formalism. We have also shown the correlation functions from our averaged simulations, for which the agreement with the PDE is excellent.

We tested our PDE approximation for the parameter space described in earlier work [15] and the further parameter investigations outlined in Sec. IV. We find that our

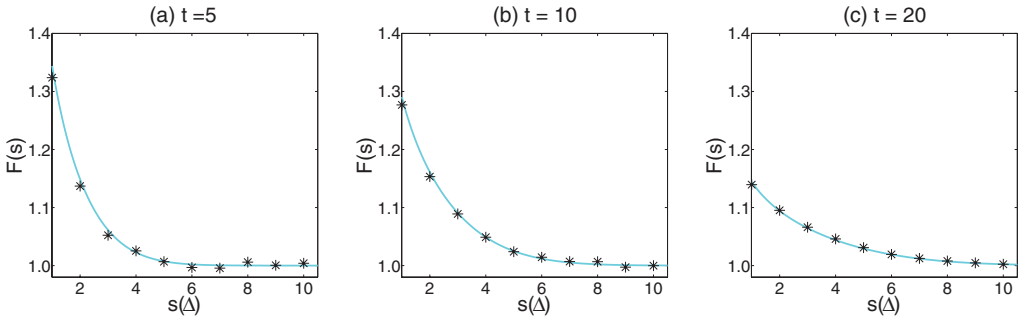

FIG. 6. (Color online) The correlation function, $F(s)$, decreases as the distance increases. Results here are for three different times all with parameters $P_m = 1$, $P_p = 0.1$, and $P_d = 0.01$. The curve in cyan (light gray) displays results from solution of the PDE, whereas the black asterisks are from averaged discrete data. The agreement between the two is very good.

approximation performs very well throughout the parameter space in which it is appropriate to close the hierarchy of correlation equations at the pair level to predict the average behavior of the IBMs.

B. Derivation in three dimensions

We derive the PDE in 3D using the same method. At the boundary, the equation for the evolution of the correlation function is

$$\frac{dF(\Delta)}{dt} = \frac{P_m}{3}[4F(\sqrt{2}\Delta) + F(2\Delta) - 5F(\Delta)] - 2P_pF(\Delta)[1 - F(\Delta)c_A] + \frac{P_p}{3c_A}[1 - c_AF(\Delta)] + \frac{P_p}{3(1-c_A)}[1 - c_AF(\Delta)]^2[4F(\sqrt{2}\Delta) + F(2\Delta)]. \tag{3.10}$$

Elsewhere, we have

$$\frac{dF(x,y,z)}{dt} = \frac{P_m}{3}[F(x+\Delta,y,z) + F(x-\Delta,y,z) + F(x,y+\Delta,z) + F(x,y-\Delta,z) + F(x,y,z+\Delta) + F(x,y,z-\Delta) - 6F(x,y,z)] - 2P_pF(x,y,z)[1 - c_AF(\Delta)] + \frac{P_p}{3(1-c_A)}[1 - c_AF(\Delta)][1 - c_AF(x,y,z)][F(x+\Delta,y,z) + F(x-\Delta,y,z) + F(x,y+\Delta,z) + F(x,y-\Delta,z) + F(x,y,z+\Delta) + F(x,y,z-\Delta)]. \tag{3.11}$$

As before, we Taylor expand around (x,y,z), keeping terms up to second order,

$$\frac{\partial F}{\partial t} = \frac{P_m\Delta^2}{3}\left[\frac{\partial^2 F}{\partial x^2} + \frac{\partial^2 F}{\partial y^2} + \frac{\partial^2 F}{\partial z^2}\right] - 2P_pF[1 - c_AF(\Delta)] + \frac{P_p}{3(1-c_A)}[1 - c_AF(\Delta)][1 - c_AF] \times \left[6F + \Delta^2\frac{\partial^2 F}{\partial x^2} + \Delta^2\frac{\partial^2 F}{\partial y^2} + \Delta^2\frac{\partial^2 F}{\partial z^2}\right] + \mathcal{O}(\Delta^3), \tag{3.12}$$

where $F = F(x,y,z)$ for clarity. From our examination of the system in 2D, we again allow $\Delta \to 0$, remembering that P_m scales with Δ^2, obtaining

$$\frac{\partial F}{\partial t} = \frac{\hat{P}_m}{3}\left[\frac{\partial^2 F}{\partial x^2} + \frac{\partial^2 F}{\partial y^2} + \frac{\partial^2 F}{\partial z^2}\right] - 2P_pF[1 - c_AF(\Delta)] + \frac{P_p}{1-c_A}[1 - c_AF(\Delta)][1 - c_AF]2F. \tag{3.13}$$

Finally, we switch to radial coordinates, noting that our system will be radially symmetric due to the homogeneous initial conditions, to arrive at

$$\frac{\partial F(s)}{\partial t} = \frac{\hat{P}_m}{3}\left(\frac{\partial^2 F(s)}{\partial s^2} + \frac{2}{s}\frac{\partial F(s)}{\partial s}\right) + 2P_pc_AF(s)[1 - c_AF(\Delta)]\left[\frac{1 - F(s)}{1 - c_A}\right], \quad s > \Delta. \tag{3.14}$$

We notice that the PDE has the same form in 2D, Eq. (3.6), and 3D, Eq. (3.14).

IV. PARAMETER INVESTIGATIONS

To add to the parameter investigation performed in Ref. [15], we also consider regions of parameter space where motility is reduced relative to proliferation. Thus, we keep P_p at unity and vary P_m and P_d accordingly. We, first, look at the case where there is no death ($P_d = 0$) and investigate different rates of movement in 2D and 3D, as seen in Fig. 7. We find that the agreement between the correlation PDE and the averaged IBM improves as the rate of movement increases. We also find that, for the same set of parameters, better agreement between the correlation equations and the averaged IBM is seen in 3D than in 2D, which agrees with the results of Ref. [15]. We find that the PDE approximation is always an improvement on the MFA.

We then allow death to occur and examine the system, finding that our correlation PDE still provides a good agreement with the averaged IBM. In Fig. 8, we show results for various movement rates in 2D and 3D, where the death rate is 40% of the proliferation rate. We note that, when death is nonzero, the MFA generally does not reach the same steady state as the averaged IBM but that the correlation PDE provides excellent agreement.

In a very small region of parameter space our simulated system quickly tends to extinction and this behavior is not reflected by either the MFA or the model with correlations included (either the ODE or PDE formulation), although inclusion of the correlations still provides a better approximation than the MFA. This can be seen in Fig. 9. We also note that it is only within this region of parameter space that our PDE approximation to the system of ODEs begins to break down; thus, we can use our PDE approximation in all regions of parameter space where it is viable to close the hierarchy of correlation equations at the pair level to predict the averaged IBM behavior. This transition from positive to vanishing steady-state densities corresponds to the state phase transition of the contact process [31,46]. This transition between absorbing and active states has been investigated analytically by series expansions [46]. In future work, we will investigate the phase transition in more detail and develop

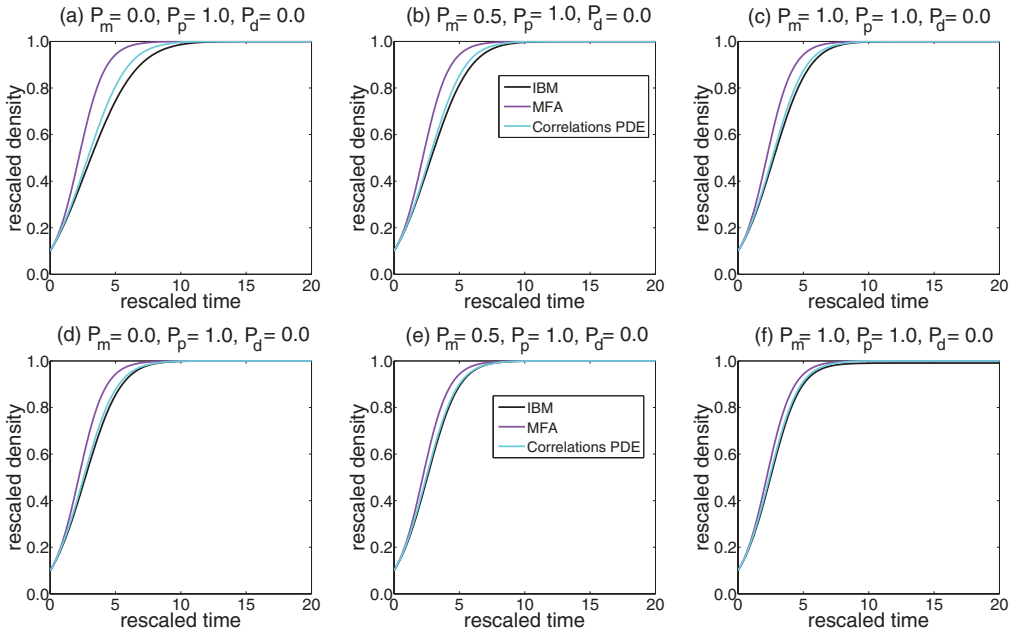

FIG. 7. (Color online) We investigate the effects on our approximation of increasing the movement rate, P_m, in 2D (top row) and 3D (bottom row) when there is no death, $P_d = 0$. An increased movement rate leads to a closer agreement between the corrected equations and the discrete behavior. The agreement also improves in higher dimensions for the same parameters. Any discrepancies observed between the correlations PDE and the averaged IBM are due to the closure approximations as discussed in Ref. [15].

methods which will produce accurate results in the regions of parameter space where extinction occurs.

V. CONCLUSIONS AND FUTURE WORK

In this work we have derived a PDE that represents the pairwise correlations in lattice site occupancies in a volume-excluding, discrete birth-death-movement process on a square lattice. Due to the nonuniformity of lattice site distances, using a system of ODEs to describe the evolution of pairwise correlation functions at every lattice distance is inconvenient as deriving the equations at the required distances and encoding them to solve numerically is time-consuming. The derivation of a PDE approximation, such as the one described in this work, makes the numerical solution of the system far more tractable because we can now solve the equations on a uniform

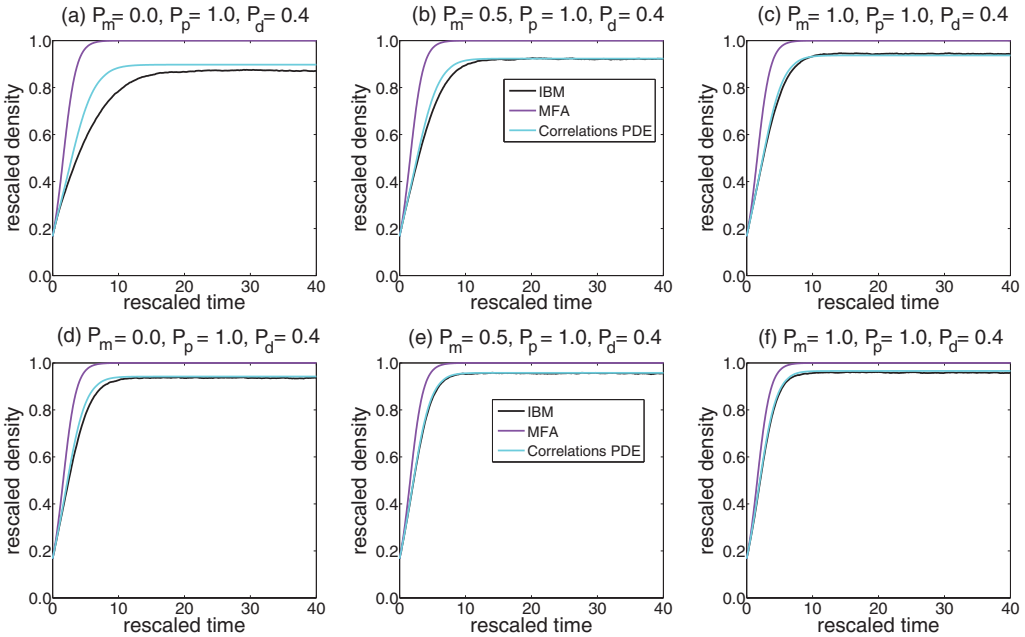

FIG. 8. (Color online) We investigate the effects on our approximation of increasing the movement rate, P_m, in 2D (top row) and 3D (bottom row) for a nonzero death rate, $P_d > 0$. An increased movement rate leads to a closer agreement between the corrected equations and the discrete behavior.

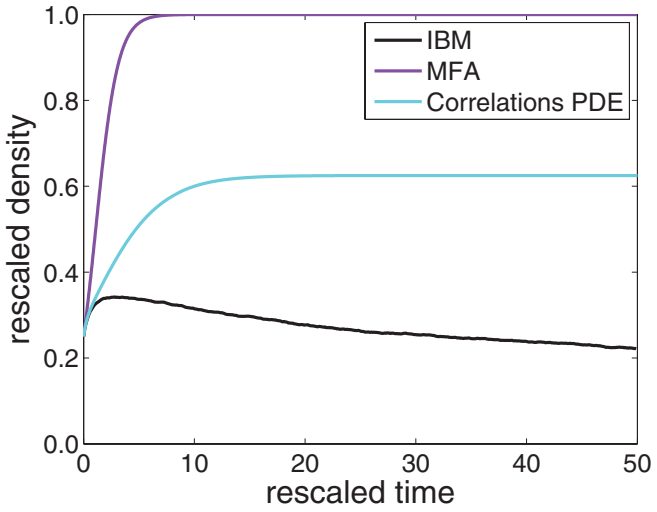

FIG. 9. (Color online) For high rates of death, P_d, we see the IBM leads to extinction. This behavior is not reflected by the MFA or the correlations PDE. Results shown here are for the 2D case with $P_m = 0.0$, $P_p = 1.0$, and $P_d = 0.6$, which shows worse agreement than the 3D case for the same parameter values.

lattice. This makes it easier to ensure we include the pairwise correlations to a sufficiently large distance before assuming independence of lattice occupancies. Moreover, using the PDE approximation makes it feasible to extend this model to more complex situations. For example, with two species, there are 3 times as many correlation ODEs (for species A and B we will have $F_{A,A}$, $F_{A,B}$, and $F_{B,B}$); thus, being able to describe the system using three coupled PDEs will be far more tractable than the equivalent system of nonuniform ODEs. Additionally, it will be useful to develop PDE approximations to deal with inhomogeneous initial conditions, as in this case rotational symmetry and translation invariance are lost and the number of correlation ODEs increases dramatically. Both of these avenues will be explored in future work.

In developing the PDE, we allowed our lattice spacing to tend to zero, as is done for cases where population-level PDEs have been derived without including the effects of correlations. This assumption may not always be valid as it is not physically realistic to assume that a cell diameter is zero. However, we find that our method works well throughout the parameter space in which correlations provide a good estimate of averaged IBM results.

We have also investigated a wider parameter space than that tested in Ref. [15]. Specifically, we investigated regions whereby motility is lowered relative to proliferation, with and without agent death. We generally find good agreement between results from our correlations PDE and the averaged IBM, in contrast to the MFA. The approximation works better for higher rates of movement. When death is present in the model, we find that the correlations PDE predicts the steady state reached in the averaged IBM very well, whereas this behavior is not captured by the MFA. However, for very high death rates, the IBM tends to extinction (the absorbing state of the contact process) without first reaching a quasisteady state. This is not reflected in our correlations PDE, although it does still provide an improvement on the MFA. In this region, an alternative method will need to be considered, and this will be the subject of our future work, as will a rigorous determination of the phase transition.

If spatial correlations are not included in population models, parameters may be inaccurately estimated from biological data [15]. The method we have presented allows spatial correlations to large distances to be easily included in models of populations undergoing birth-death-movement processes. This is important not only for predicting the system's behavior but also for estimating the model parameters from biological data [32].

ACKNOWLEDGMENTS

The authors thank Philip K. Maini for valuable comments. This research is supported by the Australian Research Council Discovery Project DP120100551 and the 2011 International Exchange Scheme funded by the Royal Society. D.C.M thanks Oxford University Press for support through the Clarendon Fund, as well as Keble College, Oxford, for support through the Sloane-Robinson award.

[1] P. C. Lai, C. M. Wong, A. J. Hedley, S. V. Lo, P. Y. Leung, J. Kong, and G. M. Leung, Environ. Health Perspect **112**, 1550 (2004).
[2] D. C. G. Law, M. L. Serre, G. Christakos, P. A. Leone, and W. C. Miller, Sex. Transm. Infect **80**, 294 (2004).
[3] Z.-W. Jia, X.-W. Jia, Y.-X. Liu, C. Dye, F. Chen, C.-S. Chen, W.-Y. Zhang, X.-W. Li, W.-C. Cao, and H.-L. Liu, Emerg. Infect. Dis. **14**, 1413 (2008).
[4] K. J. Sharkey, C. Fernandez, K. L. Morgan, E. Peeler, M. Thrush, J. F. Turnbull, and G. B. Bowers, J. Math. Biol. **53**, 61 (2006).
[5] K. J. Sharkey, Theor. Pop. Biol. **79**, 115 (2011).
[6] N. Nunan, K. Wu, I. M. Young, J. W. Crawford, and K. Ritz, Microb. Ecol. **44**, 296 (2002).
[7] Y. Jiao, H. Berman, T. Kiehl, and S. Torquato, PLOS One **6**, e27323 (2011).
[8] C. J. Kastrup, J. Q. Boedicker, A. P. Pomerantsev, M. Moayeri, Y. Bian, R. R. Pompano, T. R. Kline, P. Sylvestre, F. Shen, S. H. Leppla, W. Tang, and R. F. Ismagilov, Nat. Chem. Biol. **4**, 742 (2008).
[9] G. B. Ermentrout and L. Edelstein-Keshet, J. Theor. Biol. **160**, 97 (1993).
[10] P. Hogeweg, Appl. Math. Comp. **27**, 81 (1988).
[11] J. Moreira and A. Deutsch, Adv. Complex Syst. **05**, 247 (2002).
[12] H. Fuks and A. T. Lawniczak, Discrete Dyn. Nat. Soc. **6**, 191 (2001).
[13] D. Hiebeler, J. Theor. Biol. **187**, 307 (1997).
[14] M. A. M. de Aguiar, E. M. Rauch, and Y. Bar-Yam, J. Stat. Phys. **114**, 1417 (2004).
[15] R. E. Baker and M. J. Simpson, Phys. Rev. E **82**, 041905 (2010).
[16] N. Peyrard and A. Franc, Physica A **358**, 575 (2005).

[17] P. E. Parham and N. M. Ferguson, J. R. Soc. Interface **3**, 483 (2006).
[18] J. A. N. Filipe and G. J. Gibson, Phil. Trans. R. Soc. Lond. B **353**, 2153 (1998).
[19] S. P. Ellner, A. Sasaki, Y. Haraguchi, and H. Matsuda, J. Math. Biol. **36**, 469 (1998).
[20] M. J. Simpson and R. E. Baker, Phys. Rev. E **83**, 051922 (2011).
[21] G. Ascolani, M. Badoual, and C. Deroulers, Phys. Rev. E **87**, 012792 (2013).
[22] R. Law, D. J. Murrell, and U. Dieckmann, Ecology **84**, 252 (2003).
[23] W. R. Young, A. J. Roberts, and G. Stuhne, Nature **412**, 328 (2001).
[24] U. Dieckmann and R. Law, in *The Geometry of Ecological Interactions: Simplifying Spatial Complexity* (Cambridge University Press, Cambridge, UK, 2000), pp. 412–455.
[25] S. P. Ellner, J. Theor. Biol. **210**, 435 (2001).
[26] D. J. Murrell, U. Dieckmann, and R. Law, J. Theor. Biol. **229**, 421 (2004).
[27] M. Raghib, N. A. Hill, and U. Dieckmann, J. Math. Biol. **62**, 605 (2011).
[28] T. E. Harris, Ann. Probab. **2**, 969 (1974).
[29] T. M. Liggett, *Stochastic Interacting Systems: Contact, Voter and Exclusion Processes* (Springer, Berlin, 1999).
[30] R. Dickman, Phys. Rev. B **40**, 7005 (1989).
[31] R. Dickman, J. Stat. Phys. **55**, 997 (1989).
[32] M. J. Simpson, B. J. Binder, P. Haridas, B. K. Wood, K. K. Treloar, D. L. S. McElwain, and R. E. Baker, Bull. Math. Biol. **75**, 871 (2013).
[33] J. Smolle, F. M. Smolle-Juettner, H. Stettner, and H. Kerl, Am. J. Dermatopathol. **14**, 231 (1992).
[34] T. Czaran and S. Bartha, Trends Ecol. Evol. **7**, 38 (1992).
[35] J. Silvertown, S. Holtier, J. Johnson, and P. Dale, J. Ecol. **80**, 527 (1992).
[36] J. Mai, V. N. Kuzovkov, and W. von Niessen, J. Chem. Phys. **98**, 10017 (1993).
[37] J. Mai, V. N. Kuzovkov, and W. von Niessen, Physica A **203**, 298 (1994).
[38] A. Singer, J. Chem. Phys. **121**, 3657 (2004).
[39] W. H. Press, S. A. Teukolsky, W. T. Vetterling, and B. P. Flannery, *Numerical Recipes: The Art of Scientific Computing* (Cambridge University Press, Cambridge, UK, 2007).
[40] E. A. Codling, M. J. Plank, and S. Benhamou, J. R. Soc. Interface **5**, 813 (2008).
[41] A. Stevens and H. G. Othmer, SIAM J. Appl. Math. **57**, 1044 (1997).
[42] H. G. Othmer, S. R. Dunbar, and W. Alt, J. Math. Biol. **26**, 263 (1988).
[43] M. J. Simpson, K. A. Landman, and B. D. Hughes, Physica A **389**, 3779 (2010).
[44] M. J. Simpson, B. D. Hughes, and K. A. Landman, Australas. J. Eng. Ed. **15**(2), 59 (2009).
[45] C. Zheng and G. D. Bennett, *Applied Contaminant Transport Modeling* (Wiley-Blackwell, London, 2002).
[46] I. Jensen and R. Dickman, J. Phys. A: Math. Gen. **26**, L151 (1993).